

A ubiquitous endocrine disruptor tributyltin induces muscle wasting and retards muscle regeneration

Hsien-Chun Chiu¹, Rong-Sen Yang², Te-I Weng³, Chen-Yuan Chiu⁴, Kuo-Cheng Lan^{5*} & Shing-Hwa Liu^{1,6,7*} 

¹Institute of Toxicology, College of Medicine, National Taiwan University, Taipei, Taiwan; ²Departments of Orthopaedics, College of Medicine, National Taiwan University, Taipei, Taiwan; ³Department of Forensic Medicine, College of Medicine, National Taiwan University, Taipei, Taiwan; ⁴Center of Consultation, Center for Drug Evaluation, Taipei, Taiwan; ⁵Department of Emergency Medicine, Tri-Service General Hospital, National Defense Medical Center, Taipei, Taiwan; ⁶Department of Medical Research, China Medical University Hospital, China Medical University, Taichung, Taiwan; ⁷Department of Pediatrics, College of Medicine, National Taiwan University, Taipei, Taiwan

Abstract

Background Organotin pollutant tributyltin (TBT) is an environmental endocrine disrupting chemical and is a known obesogen and diabetogen. TBT can be detected in human following consumption of contaminated seafood or water. The decrease in muscle strength and quality has been shown to be associated with type 2 diabetes in older adults. However, the adverse effects of TBT on the muscle mass and function still remain unclear. Here, we investigated the effects and molecule mechanisms of low-dose TBT on skeletal muscle regeneration and atrophy/wasting using the cultured skeletal muscle cell and adult mouse models.

Methods The mouse myoblasts (C2C12) and differentiated myotubes were used to assess the in vitro effects of low-dose tributyltin (0.01–0.5 μ M). The in vivo effects of TBT at the doses of 5 and 25 μ g/kg/day ($n = 6$ /group), which were five times lower than the established no observed adverse effect level (NOAEL) and equal to NOAEL, respectively, by oral administration for 4 weeks on muscle wasting and muscle regeneration were evaluated in a mouse model with or without glycerol-induced muscle injury/regeneration.

Results TBT reduced myogenic differentiation in myoblasts (myotube with 6–10 nuclei: 53.9 and 35.8% control for 0.05 and 0.1 μ M, respectively, $n = 4$, $P < 0.05$). TBT also decreased myotube diameter, upregulated protein expression levels of muscle-specific ubiquitin ligases (Atrogin-1 and MuRF1), myostatin, phosphorylated AMPK α , and phosphorylated NF κ B-p65, and downregulated protein expression levels of phosphorylated AKT and phosphorylated FoxO1 in myotubes (0.2 and 0.5 μ M, $n = 6$, $P < 0.05$). Exposure of TBT in mice elevated body weight, decreased muscle mass, and induced muscular dysfunction (5 and 25 μ g/kg, $P > 0.05$ and $P < 0.05$, respectively, $n = 6$). TBT inhibited soleus muscle regeneration in mice with glycerol-induced muscle injury (5 and 25 μ g/kg, $P > 0.05$ and $P < 0.05$, respectively, $n = 6$). TBT upregulated protein expression levels of Atrogin-1, MuRF1, myostatin, and phosphorylated AMPK α and downregulated protein expression level of phosphorylated FoxO1 in the mouse soleus muscles (5 and 25 μ g/kg, $P > 0.05$ and $P < 0.05$, respectively, $n = 6$).

Conclusions This study demonstrates for the first time that low-dose TBT significantly inhibits myogenic differentiation and triggers myotube atrophy in a cell model and significantly decreases muscle regeneration and muscle mass and function in a mouse model. These findings suggest that low-dose TBT exposure may be an environmental risk factor for muscle regeneration inhibition, atrophy/wasting, and disease-related myopathy.

Keywords Tributyltin; Environmental pollutants; Muscle regeneration; Muscle wasting

Received: 10 May 2022; Revised: 14 September 2022; Accepted: 10 October 2022

*Correspondence to: Shing-Hwa Liu, Institute of Toxicology, College of Medicine, National Taiwan University, Taipei, Taiwan. Email: shinghwaliu@ntu.edu.tw;

Kuo-Cheng Lan, Department of Emergency Medicine, Tri-Service General Hospital, National Defense Medical Center, Taipei, Taiwan. Email: kclan.tw@yahoo.com.tw

Hsien-Chun Chiu, Rong-Sen Yang, and Te-I Weng contributed equally to this study.

Introduction

Environmental endocrine disrupting chemicals (EDCs) can adversely affect human and wildlife populations that can interfere in the endocrine system and cause harmful effects.¹ The experimental and epidemiological studies have demonstrated that EDCs are associated with metabolic diseases, such as obesity, metabolic syndrome, diabetes mellitus, and non-alcoholic fatty liver disease.¹ There is growing evidence that loss of muscle strength and mass is associated with metabolic diseases such as type 2 diabetes in older adults.² Cigarette smoke is known to contain EDCs. Maternal smoking during pregnancy has been shown to have a low birth weight, which in turn increases the risk of obesity.³ EDCs, such as bisphenol-A, phthalates, and perfluoroalkyl acids, have been implicated in foetal growth retardation and low birth weight.⁴ A previous study showed that, in young men with low birth weight, the composition and size of skeletal muscle fibres were altered prior to whole-body insulin resistance.⁵ The adverse effects of environmental EDCs exposure on myogenesis and muscle mass are worth further investigation.

Tributyltin (TBT) is one of the most widespread EDCs.^{1,6} TBT is the main organotin species used as polyvinyl chloride heat stabilizers, biocide, wood preservatives, and antifouling paints. The characteristics of low solubility, lipophilic, and high gravity make it easy to present in marine aquatic organisms or bonds to sediment for a long time.⁶ Even though TBT antifouling paints are banned by international agencies, a previous study has shown that the detected levels of butyltin compounds (maximum total concentrations of fish muscles and livers were 715 and 1132 ng Sn/g, respectively) are still higher in muscle and liver tissues of fishes from the Polish coast of the Baltic Sea after 6–7 years of the implementation of ban regulation.⁷ An experiment study on Atlantic salmon (*Salmo salar*) from farms using TBT-treated nets showed the increased accumulation of TBT (500–1000 µg/kg) in muscle tissues.⁸ Moreover, the occurrence of organotins has also been demonstrated in house dust samples from Berlin (Germany) and Albany (New York, USA).^{9,10} Therefore, human can exposure to organotin through ingestion of contaminated seafood, water, or house dust.^{7–10} The levels of total butyltin in human blood samples have been detected to be ranging from less than the limit of detection to 101 ng/mL.¹¹ TBT is a known obesogen and diabetogen.^{1,4,6} Several animal studies have found that TBT at the environmentally relevant doses (0.05–500 µg/kg) can affect fat deposition, oestrogen-receptor interaction, and glucose homeostasis.^{1,12,13} Furthermore, several studies showed that exposure of pregnant rats to organotin caused the reduction of birth weight.^{14–16} The adverse effects of TBT on muscle regeneration and wasting/atrophy are still unclear.

This study hypothesized that low-dose TBT could effectively not only retard muscle regeneration but also in-

duce muscle wasting/atrophy. We used a well-established myoblast cell models to investigate the in vitro effects of TBT on myogenic differentiation and differentiated myotube atrophy. A previous study showed that the detectable concentrations of human blood TBT ranged from 2.4 to 85 ng/mL (8.27–293 nM).¹¹ Therefore, TBT at the concentrations of 0.01–0.5 µM was used in this study for in vitro experiments. A well-established mouse model with or without glycerol-induced muscle injury/regeneration to test the in vivo effects of TBT on muscle wasting and muscle regeneration. The value of tolerable daily intake (TDI) for TBT has been established to be 0.25 µg/kg/day based on the no observed adverse effect level (NOAEL) of 25 µg/kg/day in the long-term animal toxicity studies, resulted in a safety factor of 100.¹⁷ Therefore, TBT at the doses of 5 and 25 µg/kg/day, which were five times lower than the established NOAEL and equal to NOAEL, respectively, was used in this study for in vivo experiments.

Materials and methods

Detailed descriptions of materials and methods were shown in Supporting information, Data S1.

C2C12 mouse myoblasts and myoblast differentiation and myotube formation

C2C12 myoblasts were cultured onto 6-well plates containing growth medium (GM) for one day, and then cultured into differentiation medium (DM) contained nutrient mixture F-12K Ham solution/MCDB201 (1:1) with 2% horse serum for 4 days and replaced every 24 h with or without TBT (0.01–0.1 µM) during myoblast differentiation period.

Morphological analysis in myotubes

The observable characteristics of myotube formation and myotube atrophy were examined by analysis of multinucleated myotube formation and diameters from the widest part of multinucleated myotubes with haematoxylin and eosin (H&E) staining under an optical Nikon Eclipse TS100 microscope equipped with a Nikon D5100 digital camera. During myoblast differentiation, myotubes were calculated by the frequency distribution of myotube nuclei (2–5, 6–10, and >10 nuclei). In well-differentiated myotubes, myotubes were calculated by the frequency distribution of myotube diameter (<15, 15–30, >30 µm).

Animals

Male ICR mice (6-week-old) were purchased from the Animal Center of the College of Medicine, National Taiwan University (IACUC Approval No: 20201066) and housed under controlled environmental conditions ($22 \pm 2^\circ\text{C}$, per 12 h light/dark cycle) with food and water *ad libitum*. Animals were allowed to acclimate for 1 week prior to research use. Mice were randomly divided into seven groups ($n = 6/\text{group}$): normal control mice, mice with TBT (5 and 25 $\mu\text{g}/\text{kg}$) treatment, sham control for glycerol injection, normal mice with glycerol injection, and TBT (5 and 25 $\mu\text{g}/\text{kg}$)-treated mice with glycerol injection. TBT chloride (Sigma Aldrich, St. Louis, MO, USA) was dissolved in corn oil. During the period of experiment, mice were orally administered with corn oil or TBT via a gavage needle once every day for 4 weeks (ages of mice: 11-week-old). At the end of the experiment, mice were fasted for 12 h with water *ad libitum*. The blood samples were collected from tail veins, and then the blood glucose was measured using an Anstense-III glucose analyzer (Horiba, Kyoto, Japan). The plasma insulin was determined by an insulin antiserum immunoassay (Mercodia, Uppsala, Sweden). The operators who performed the data collection/analysis were blinded.

Muscle regeneration model in mice

The glycerol-induced muscle injury-regeneration model was performed as previously described.^{18,19} Mice were anaesthetised and glycerol (100 μL of 50%, *v/v*) was injected into soleus muscles. After 5 days of glycerol injection, soleus muscles were isolated after mouse euthanasia. The 5- μm tissue slices were prepared for histological analysis.

Muscle fatigue task

The muscular endurance was measured by the rotarod apparatus as previously described.^{18,19} Briefly, mice were acclimated to training before the fatigue task performed in an accelerating rotarod (Ugo Basile, Varese, Italy).

Grip strength test

The muscle strength was measured by a grip strength device (DTG-2, Bio-Cando, Taoyuan, Taiwan). The muscle strength of both forelimb and hindlimb was recorded. The grip strength test of each mouse was repeated five times.

Sampling

The skeletal muscles (soleus, tibialis anterior, gastrocnemius, and extensor digitorum longus) were dissected,

harvested, weighted, and prepared for following histological and immunohistochemical analysis. Some muscle samples were stored in -20°C for following Western blotting.

Histological and immunohistochemical analysis

The analysis of histology and immunohistochemistry was determined as previously described.^{18,19} The soleus muscles were dissected from hind limbs and then fixed in 4% paraformaldehyde. The cross-sections (5 μm) of paraffin-embedded muscle tissues were used for H&E staining and immunohistochemistry. The CSA and myofibres were assessed through high-powered field with an optical Nikon Eclipse TS100 microscope equipped with a Nikon D5100 digital camera and calculated using the image J 1.48 software (National Institutes of Health) in five random fields of each section per mouse. The CSA was calculated by mean of 150–250 fibres for each section. For immunohistochemistry (IHC), slices were dewaxed, rehydrated, and blocked, and then incubated with primary antibodies overnight. Haematoxylin was used to counterstain the sections. The semi-quantitative IHC was determined by the ImageJ Fiji 1.2 software.²⁰

Immunoblotting

Equal amounts of proteins (10–30 μg) were separated on SDS-PAGE and electrotransferred to the polyvinylidene difluoride (PVDF) membranes. Membranes were washed with 0.2% TBST followed by blocking with 5% skim milk for 1 h and subsequently incubated with primary antibodies with 1:2000 dilution at 4°C overnight. PVDF membranes were then incubated with corresponding secondary antibodies for 1 h at room temperature. Finally, the membranes were washed and then treated with enhanced chemiluminescence reagent (Bio-Rad Laboratories, Redmond, WA, USA) and visualized on the Fujii X-ray film.

Statistics

The one-way analysis of variance (ANOVA) and unpaired two-tailed Student's *t*-test was used for comparison among different groups. For analysing distribution of myofibre sizes, the two-way ANOVA followed by post hoc analysis with the Sidak test was performed. The *P* value less than 0.05 was considered to be statistically significant. Statistical analysis was performed by GraphPad Prism 6.

Results

Low-dose TBT inhibits myogenesis and regulates related signalling molecules in a myoblast cell model.

We first investigated whether low-concentration TBT caused inhibition of myogenic differentiation in C2C12 myoblasts. As shown in *Figure 1A,B-a*, TBT (0.01–0.1 μM) treatment significantly inhibited the multinucleated myotube formation, which the frequent distribution of nuclei at 6–10

and >10 unit was affected, in myoblasts subjected to 4 days of differentiation (0.1 μM , 6–10 unit, $P = 0.002$, >10 unit, $P < 0.001$; 0.05 μM , >10 unit, $P = 0.003$; 0.01 μM , >10 unit, $P = 0.019$, vs. control). The total differentiated myotube numbers were also significantly reduced by TBT treatment at a concentration of 0.1 μM (*Figure 1B-b*; $P = 0.031$, vs. control).

TBT (0.05 and 0.1 μM) significantly downregulated the protein expression of myogenin (*Figure 2A*; 0.05 and 0.1 μM , $P = 0.018$ and $P = 0.004$; vs. DM control, respectively) and

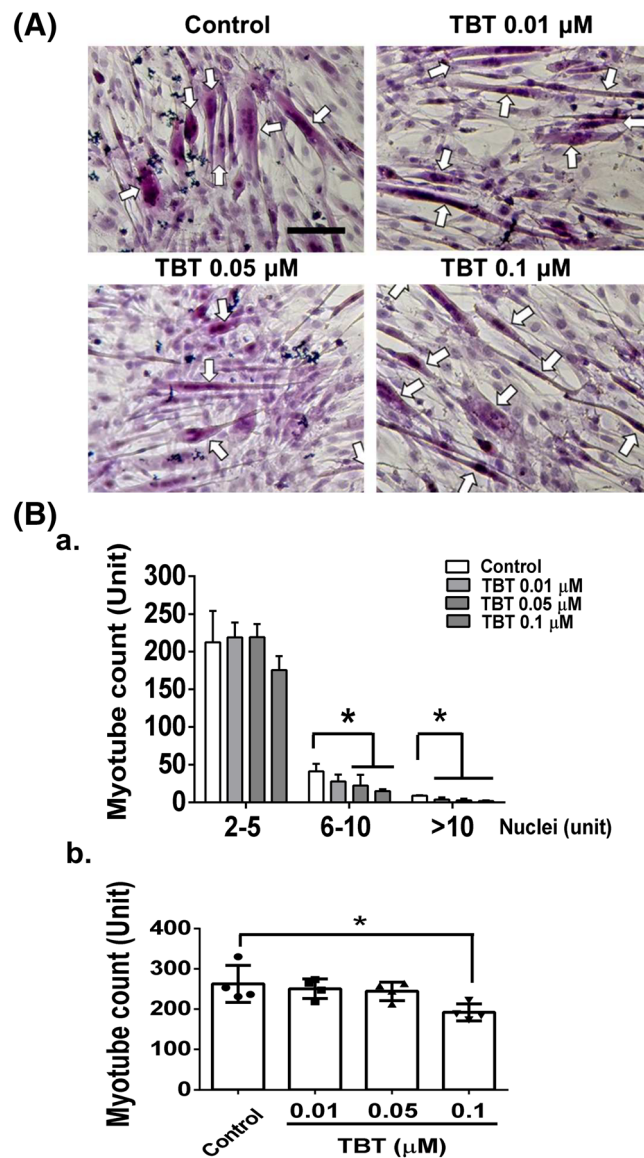


Figure 1 Effects of tributyltin (TBT) treatment on myogenic differentiation in C2C12 myoblasts during myogenic differentiation. C2C12 myoblasts were cultured in growth medium (GM) or differentiation medium (DM) for 4 days with or without TBT (0.01–0.1 μM) treatment. (A) The representative haematoxylin and eosin (H&E) stained myotube formation during myogenic differentiation of C2C12 myoblasts. Open arrows indicated the multi-nuclei myotubes. Scale bar = 100 μm . (B) Myotubes were calculated by the frequency distribution of myotube nuclei (2–5, 6–10, >10 nuclei) (a) and the number of myotube formed per field (b). There are approximately 300 myoblasts/group/biological replicate analysed. All data are presented as mean \pm SD for at least three independent experiments. The statistical analysis was performed using one-way ANOVA followed by unpaired two-tailed Student's *t*-test; for frequency distribution, two-way ANOVA followed by Sidak test was used (* $P < 0.05$ compared with control in DM without TBT treatment).

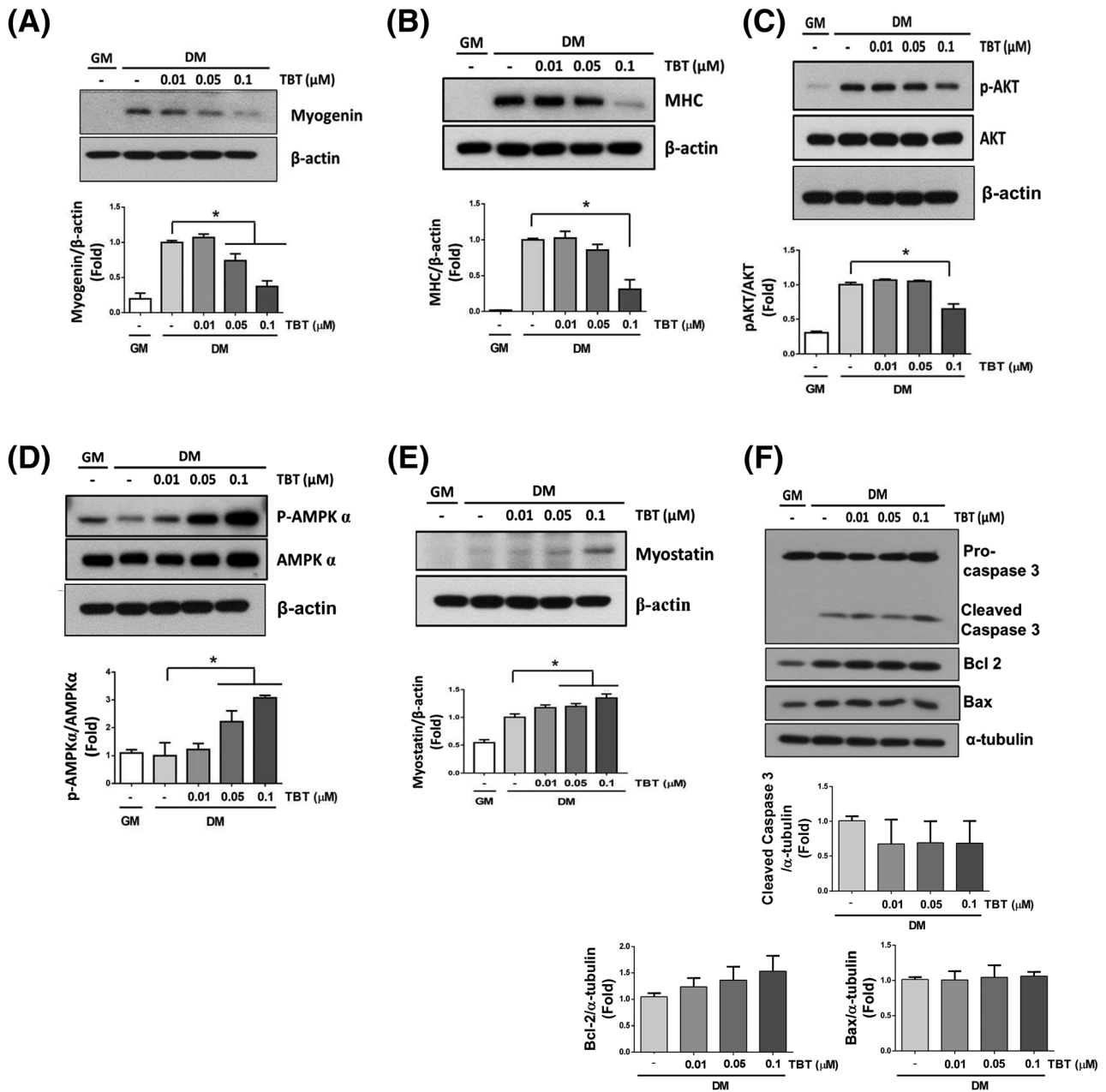


Figure 2 Effects of tributyltin (TBT) treatment on protein expression of myogenesis-related molecules and regulated signalling molecules in C2C12 myoblasts during myogenic differentiation. C2C12 myoblasts were cultured in growth medium (GM) or differentiation medium (DM) for 4 days with or without TBT (0.01–0.1 μ M) treatment. The protein expression levels for myogenin (A), myosin heavy chain (MHC; B), phosphorylated AKT (C), phosphorylated AMPK α (D), myostatin (E), caspase-3, Bcl-2, and Bax (F) were shown. The protein expression was determined by Western blotting and quantified using densitometric analysis. The β -actin was regarded as a loading control. All data are presented as mean \pm SD for at least three independent experiments. The statistical analysis was performed using one-way ANOVA followed by unpaired two-tailed Student's *t*-test.

myosin heavy chain (MHC) (the myogenesis markers) (Figure 2B; $P = 0.04$ and $P = 0.019$; vs. DM control, respectively). TBT 0.1 μ M, but not 0.05 μ M, significantly downregulated the protein expression of phosphorylated AKT (a positive regulator of myogenesis) (Figure 2C; $P > 0.05$ at 0.05 μ M and $P = 0.01$ at 0.1 μ M vs. DM control). TBT (0.05 and 0.1 μ M) significantly upregulated the protein expression of phosphor-

ylated AMPK (Figure 2D; 0.05 and 0.1 μ M, $P = 0.048$ and $P = 0.004$, vs. DM control, respectively) and myostatin (the negative regulators of myogenesis) (Figure 2E; 0.05 and 0.1 μ M, $P = 0.039$ and $P = 0.022$, vs. DM control, respectively) during myogenic differentiation in myoblasts. Moreover, TBT (0.01–0.1 μ M) did not affect the protein expression of apoptotic markers cleaved caspase-3, Bcl-2, and Bax during

myogenic differentiation in myoblasts (Figure 2F; $P > 0.05$, vs. DM control). These results suggest that low-dose TBT may have inhibitory potential on myogenesis or muscle regeneration.

Low-dose TBT induces myotube atrophy and regulates related signalling molecules in a myoblast-derived myotube model

We next investigated the effects of low-concentration TBT on myotube atrophy. C2C12 myoblasts were induced to differentiate into myotube, which was as a generally applied model of muscle atrophy *in vitro*. Our preliminary tests showed that the induction of myotube atrophy required higher concentrations of TBT than that on myogenic differentiation inhibition. Thus, the concentrations of 0.1–0.5 μM of TBT were used for myotube atrophy experiments. As shown in Figure 3A,B-a, TBT dose-dependently induced morphology alteration and diameter reduction in C2C12 differentiated myotubes after 24 h treatment. The amounts of myotubes with diameter over 30 μm were significantly reduced by 0.2 and 0.5 μM TBT treatment (Figure 3B-a; $P = 0.013$ and $P = 0.004$, respectively). The total numbers of myotubes could also be significantly decreased by 0.5 μM TBT treatment (Figure 3B-b; $P < 0.001$, vs. control).

The muscle RING finger-1 (MuRF1) and muscle atrophy F-box (Atrogin-1), the muscle-specific E3 ubiquitin ligases, are involved in the regulation of skeletal muscle mass that these ligases are required for muscle atrophy and dramatically expressed in many muscle-wasting conditions.^{19,21–23} After treatment with low-dose TBT (0.1–0.5 μM) in myotubes for 24 h, the levels of protein expression of Atrogin-1 (Figure 3C-a; 0.2 and 0.5 μM , $P = 0.001$ and $P < 0.001$, vs. control, respectively) and MuRF1 (Figure 3C-b; 0.2 and 0.5 μM , $P = 0.005$ and $P < 0.001$, vs. control, respectively) were significantly increased in a dose-dependent manner. We further tested the upstream regulatory signalling molecules of muscle-specific E3 ubiquitin ligases, including AMPK, myostatin, FoxO1, and NF- κB .^{21–23} As shown in Figure 3D,E, TBT (0.1–0.5 μM) dose-dependently and significantly upregulated the protein expression of phosphorylated AMPK α , myostatin, and phosphorylated NF- κB -p65 and downregulated the protein expression of phosphorylated FoxO1 in myotubes (0.2 and 0.5 μM : Figure 3D-a, p-AMPK α , $P < 0.001$ and $P < 0.001$; Figure 3D-b, myostatin, $P = 0.021$ and $P < 0.001$; Figure 3E-a, p-FoxO1, $P = 0.001$ and $P < 0.001$; Figure 3E-b, p-p65, $P = 0.003$ and $P < 0.001$, vs. control, respectively). Transcription factor FoxO1 is a negative regulator of muscle growth in which dephosphorylation of FoxO1 leads to nuclear entry and growth suppression.²³ The decreased phosphorylated FoxO1 reflected more FoxO1 nuclear entry to trigger Atrogin-1 and MuRF1 expression. Moreover, TBT at the concentration of 0.5 μM significantly increased the

protein expression of apoptotic markers cleaved caspase-3 and Bax, and significantly decreased the Bcl-2 protein expression in myotubes (Figure 3F; $P < 0.05$, vs. control). The amounts of myotubes with diameter over 30 μm were significantly reduced by 0.2 and 0.5 μM TBT treatment (Figure 3B-a). Therefore, 0.5 μM TBT may induce both myotube atrophy and degeneration.

Atrophic stress-induced inhibition in PI3K/AKT signalling leads to activation of FoxO transcription factors and Atrogin-1 induction in myotubes, which can be reversed by IGF-1 treatment or AKT overexpression.²³ We next investigated the role of AKT in TBT-induced myotube atrophy. As shown in Figure 4A-a,b, TBT (0.1–0.5 μM) dose-dependently and significantly decreased the AKT phosphorylation and its downstream signal mTOR phosphorylation in myotubes (0.2 and 0.5 μM : p-AKT, $P = 0.007$ and $P < 0.001$; p-mTOR, $P = 0.009$ and $P = 0.004$, vs. control, respectively). Pretreatment with SC79, an AKT activator, effectively and significantly reversed the decreased AKT phosphorylation and the increased Atrogin-1 and MuRF1 protein expression in TBT-treated myotubes (Figure 4B,C; 0.2 μM , p-AKT, $P = 0.046$ vs. control, $P = 0.025$ vs. TBT alone; Atrogin-1, $P = 0.024$ vs. control, $P = 0.005$ vs. TBT alone; MuRF1, $P = 0.005$ vs. control, $P = 0.003$ vs. TBT alone). Moreover, the myotube loss by TBT at the concentration of 0.5 μM could also be reversed by SC79 (Figure S1). Taken together, these results reveal that low-dose TBT may have potential on myotube or muscle atrophy/wasting induction.

Exposure to TBT results in skeletal muscle mass loss, dysfunction, and low regenerative capacity in a mouse model

We next investigated the *in vivo* effects of biologically relevant dose of TBT (5 and 25 $\mu\text{g}/\text{kg}$) treatment for 4 weeks on muscle mass and function in mice. The results showed that the body weights were significantly increased by TBT at a dose of 25 $\mu\text{g}/\text{kg}$, but not 5 $\mu\text{g}/\text{kg}$, from week 2 to week 4 ($P = 0.044$, 25 $\mu\text{g}/\text{kg}$ group vs. control group at Week 4; Table 1 and Figure S2A). Both TBT 5 and 25 $\mu\text{g}/\text{kg}$ treatment did not affect the food intake weekly ($P > 0.05$; Table 1 and Figure S2B). The weights of soleus, gastrocnemius, tibialis anterior, and extensor digitorum longus muscles were also measured. As shown in Table 1, the muscle weights of soleus, tibialis anterior, and extensor digitorum longus, but not gastrocnemius, significantly decreased in TBT 25 $\mu\text{g}/\text{kg}$ -treated mice compared with control mice. Treatment of TBT 5 $\mu\text{g}/\text{kg}$ did not change the weights of these four types of muscles (Table 1). Moreover, hyperglycaemia has been suggested to be a risk factor for skeletal muscle atrophy.^{18,24} TBT exposure has been shown to interfere with glucose homeostasis.^{16,17} Thus, we measured fasting blood glucose levels in mice after low-dose TBT treatment. As shown in Table 1, treatment of

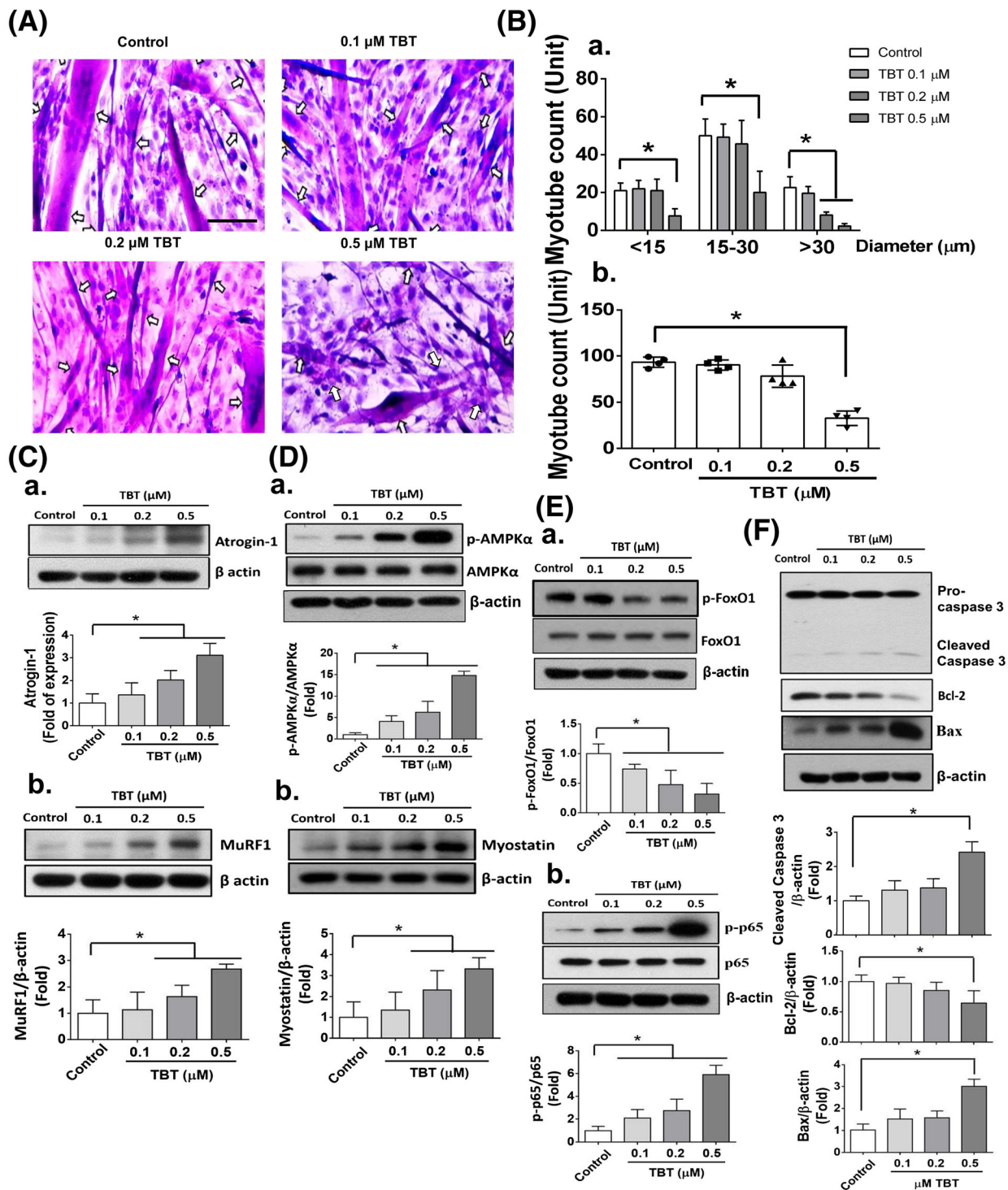


Figure 3 Effects of TBT treatment on myotube loss and atrophy and protein expression of atrophy-related signalling molecules in C2C12 myotubes. C2C12 myoblasts were cultured in differentiation medium for 4 days to form myotubes, followed by an additional 24 h with TBT (0.1–0.5 μM). (A) The representative H&E stained C2C12 myotubes were shown. The open arrows indicated the multi-nuclei myotubes. Scale bar = 100 μm. (B) Myotubes were calculated by the frequency distribution of myotube diameter (<15, 15–30, >30 μm) (A) and the number of myotube formed per field (B). There are approximately 100 multinucleated myotubes/group/biological replicate analysed. Moreover, Western blot analysis for protein expression of Atrogen-1 (C-a), MuRF1 (C-b), phosphorylated AMPKα (D-a), myostatin (D-b), phosphorylated FoxO1 (E-a), phosphorylated NF-κB-p65 (E-b), caspase-3, Bcl-2, and Bax (F) in myotubes was shown. All data are presented as mean ± SD for at least three independent experiments. The statistical analysis was performed using one-way ANOVA followed by unpaired two-tailed Student’s *t*-test; for frequency distribution, two-way ANOVA followed by Sidak test was used (**P* < 0.05 compared with control group).

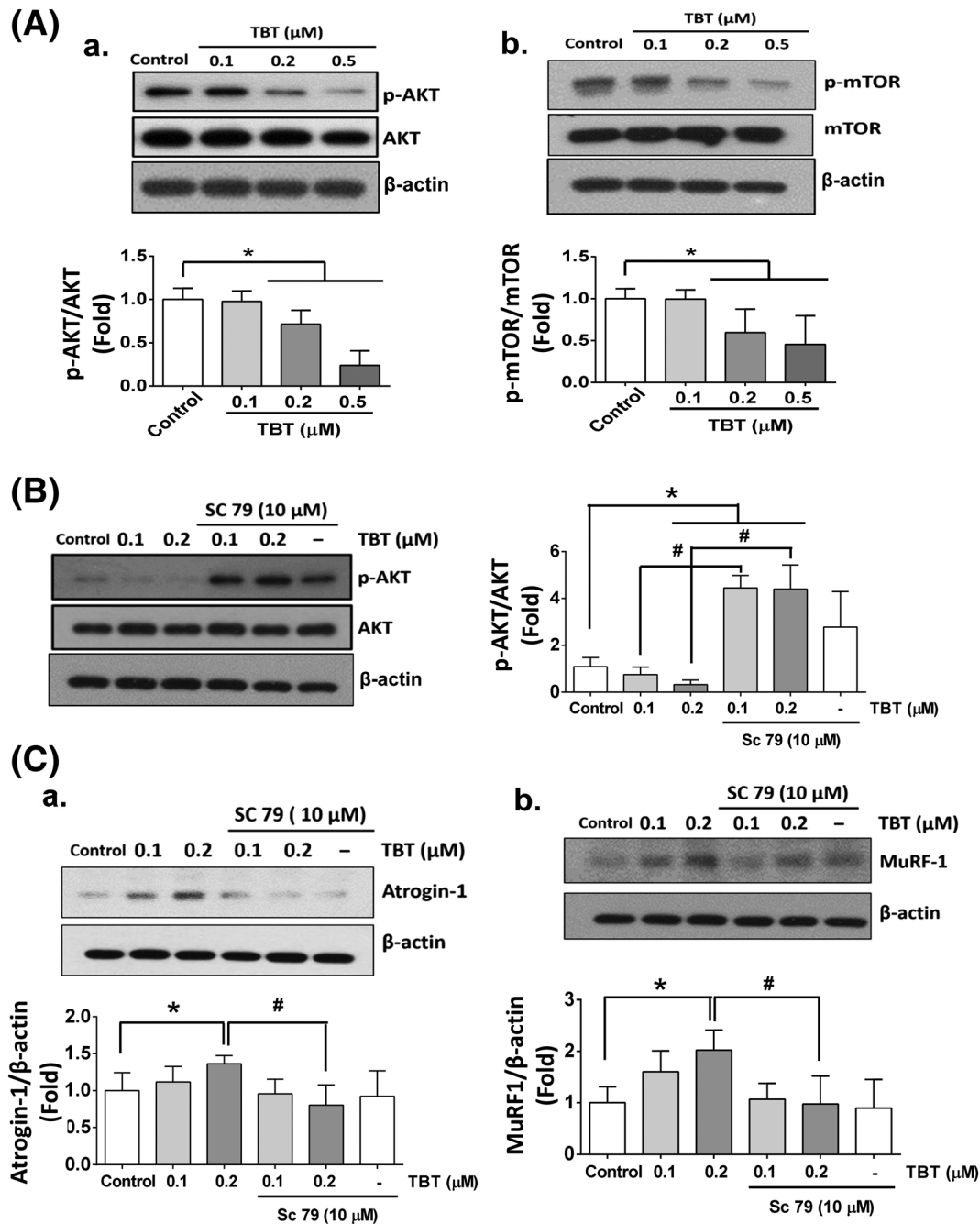


Figure 4 The role of AKT in TBT-induced myotube atrophy. C2C12 myoblast were cultured in differentiation medium for 4 days to form myotubes, followed by an additional 24 h with TBT (0.1–0.5 μM) in the presence or absence of AKT activator SC 79. (A) The protein expression of phosphorylated AKT (a) and phosphorylated mTOR (b) in TBT-treated myotubes was shown. The protein expression of phosphorylated AKT (B), Atrogin-1 (C-a), and MuRF1 (C-b) in TBT-treated myotubes with or without SC 79 treatment was shown. Data are presented as mean \pm SD for at least three independent experiments. The statistical analysis was performed using one-way ANOVA followed by unpaired two-tailed Student's *t*-test (**P* < 0.05 compared with control group. #*P* < 0.05 compared with TBT alone).

TBT 25 $\mu\text{g}/\text{kg}$, but not 5 $\mu\text{g}/\text{kg}$, significantly exhibited an elevation of blood glucose level and a decrease of plasma insulin level in mice. TBT at the doses of 5 and 25 $\mu\text{g}/\text{kg}$ did not affect the relative liver or kidney weight (5 $\mu\text{g}/\text{kg}$ TBT slightly but significantly decreased kidney weight; Table 1).

We next assessed the myofibre cross-sectional area (CSA) in soleus muscles. As shown in Figures 5A,B-a and S3A, TBT exposure was characterized by a significant reduction in the average soleus myofibre CSA in mice treated with TBT 25 $\mu\text{g}/\text{kg}$, but not 5 $\mu\text{g}/\text{kg}$, compared with the control mice

Table 1 Effects of tributyltin (TBT) on the body weight, food intake, muscle weight, and blood glucose in mice

Parameters	Control	TBT 5 µg/kg	TBT 25 µg/kg
Final body weight (g)	35.78 ± 1.03	41.58 ± 5.74 (<i>P</i> = 0.057)	38.34 ± 2.17* (<i>P</i> = 0.044)
Food intake (g/day)	49.92 ± 25.95	52.29 ± 20.42 (<i>P</i> = 0.907)	43.43 ± 16.62 (<i>P</i> = 0.734)
Muscle weight (mg/g b.w.)			
Soleus muscle	0.63 ± 0.02	0.58 ± 0.01 (<i>P</i> = 0.102)	0.55 ± 0.02* (<i>P</i> = 0.036)
Gastrocnemius	9.01 ± 0.34	8.84 ± 0.17 (<i>P</i> = 0.660)	8.66 ± 0.18 (<i>P</i> = 0.385)
Tibialis anterior	3.20 ± 0.09	2.96 ± 0.11 (<i>P</i> = 0.128)	2.93 ± 0.07* (<i>P</i> = 0.044)
Extensor digitorum longus	0.62 ± 0.01	0.57 ± 0.02 (<i>P</i> = 0.058)	0.56 ± 0.018* (<i>P</i> = 0.012)
Blood glucose (mg/dL)	90.50 ± 8.74	107.80 ± 10.04 (<i>P</i> = 0.222)	136.70 ± 14.63* (<i>P</i> = 0.022)
Blood insulin (pM)	234.1 ± 18.19	225.5 ± 11.08 (<i>P</i> = 0.695)	160.0 ± 14.87* (<i>P</i> = 0.010)
Liver weight (mg/g b.w.)	37.03 ± 1.194	34.65 ± 0.6638 (<i>P</i> = 0.111)	37.54 ± 0.8134 (<i>P</i> = 0.731)
Kidney weight (mg/g b.w.)	13.73 ± 0.3942	12.48 ± 0.2373* (<i>P</i> = 0.022)	13.48 ± 0.4140 (<i>P</i> = 0.661)

Note: Data are presented as mean ± SD (*n* = 6).

**P* < 0.05 versus control.

(*P* = 0.048, 25 µg/kg group vs. control group). Even though the distribution of myofibre CSA at 600–1200 µm² in TBT (5 and 25 µg/kg)-treated mice was significantly more abundant than control mice; however, the myofibre CSA at 1200–2000 and >2000 µm in TBT (25 µg/kg)-treated mice was significantly fewer than control mice (*P* < 0.05; Figures 5B-b and S3B).

To further determine whether the muscular function was affected by exposure to low-dose TBT, muscle fatigue task and grip strength tests were performed in mice with or without TBT treatment. TBT 25 µg/kg treatment caused a significant decrease in the forelimb grip strength in mice (*P* = 0.016; Figure S4A); both 5 and 25 µg/kg TBT treatment significantly reduced the hindlimb grip strength in mice (5 and 25 µg/kg, *P* = 0.01 and *P* < 0.001, vs. control, respectively; Figure 5C-a). Treatment of TBT 25 µg/kg, but not 5 µg/kg, significantly suppressed the muscle endurance in mice (*P* = 0.022, 25 µg/kg group vs. control group; Figure 5C-b). These in vivo results suggest that continuous exposure to low-dose TBT may impair muscle mass and muscle function.

To assess the effects of TBT exposure on regenerative capacity, glycerol was injected into the soleus muscles of mouse hind leg to induce muscle injury. An increase in the centrally nucleated myofibres characterized as early regenerating myofibres was also manifested in glycerol-injured mice, which could be significantly decreased by TBT 25 µg/kg, but not 5 µg/kg, treatment (*P* = 0.014, 25 µg/kg group vs. control; Figure 6A-a,b). Moreover, a significant reduction in the myofibre CSA of soleus muscles was observed in glycerol-injured mice, which could be significantly exacerbated by TBT 25 µg/kg, but not 5 µg/kg, treatment (*P* = 0.001, 25 µg/kg group vs. control; Figures 6A-c and S3A). The myofibre CSA at 1200–2000 and >2000 µm in TBT (5 and 25 µg/kg)-treated mice was significantly fewer than control glycerol-injured mice (*P* < 0.05; Figures 6A-d and S3B). Moreover, at 5 days after injury, a decrease in the hindlimb (Figure 6B), but not forelimb (Figure S4B), grip strength was detected in glycerol-injured mice, which could be significantly aggravated by TBT 25 µg/kg, but not 5 µg/kg,

kg, treatment (*P* = 0.033, 25 µg/kg group vs. control). These results demonstrate that low-dose TBT can induce muscle mass loss and retard muscle regeneration in vivo.

Exposure to TBT induces the muscle atrophy-related signals in a mouse model

We next investigated whether TBT induced the muscle atrophy-related signals in soleus muscles. In an immunohistochemistry analysis, the soleus muscle isolated from TBT (25 µg/kg)-treated mice exhibited an increase in atrophy accompanying with the increased protein expression of phosphorylated AMPKα, myostatin, Atrogin-1, and MuRF1 (*P* < 0.001 for these four signalling molecules; Figures 7A, B). In an immunoblotting analysis, mice continuous daily exposure to TBT 25 µg/kg for 4 weeks significantly increased the protein expression of phosphorylated AMPKα, myostatin, and major atrogene markers Atrogin-1 and MuRF1 in mouse soleus muscles (p-AMPK, *P* = 0.01; myostatin, *P* = 0.026; Atrogin-1, *P* = 0.014; MuRF1, *P* = 0.001, vs. control; Figure 7C-a-d). Moreover, the protein expression of signalling molecules for phosphorylated NF-κB-p65 and phosphorylated FoxO1 were significantly upregulated and downregulated, respectively, in soleus muscles of TBT 25 µg/kg-treated mice (p-p65, *P* = 0.041; p-FoxO1, *P* = 0.002, vs. control; Figure S5). However, the protein expression of phosphorylated AKT was not changed in soleus muscles of TBT 25 µg/kg-treated mice (*P* > 0.05 vs. control; Figure 7C-e). These results suggest that exposure to low-dose TBT in mice may induce an AMPK-mediated pathway, leading to induction of muscle wasting and weakness.

Discussion

TBT is one of the most widespread EDCs and can be a risk in the reduction of birth weight.^{14–16} Here, TBT at the

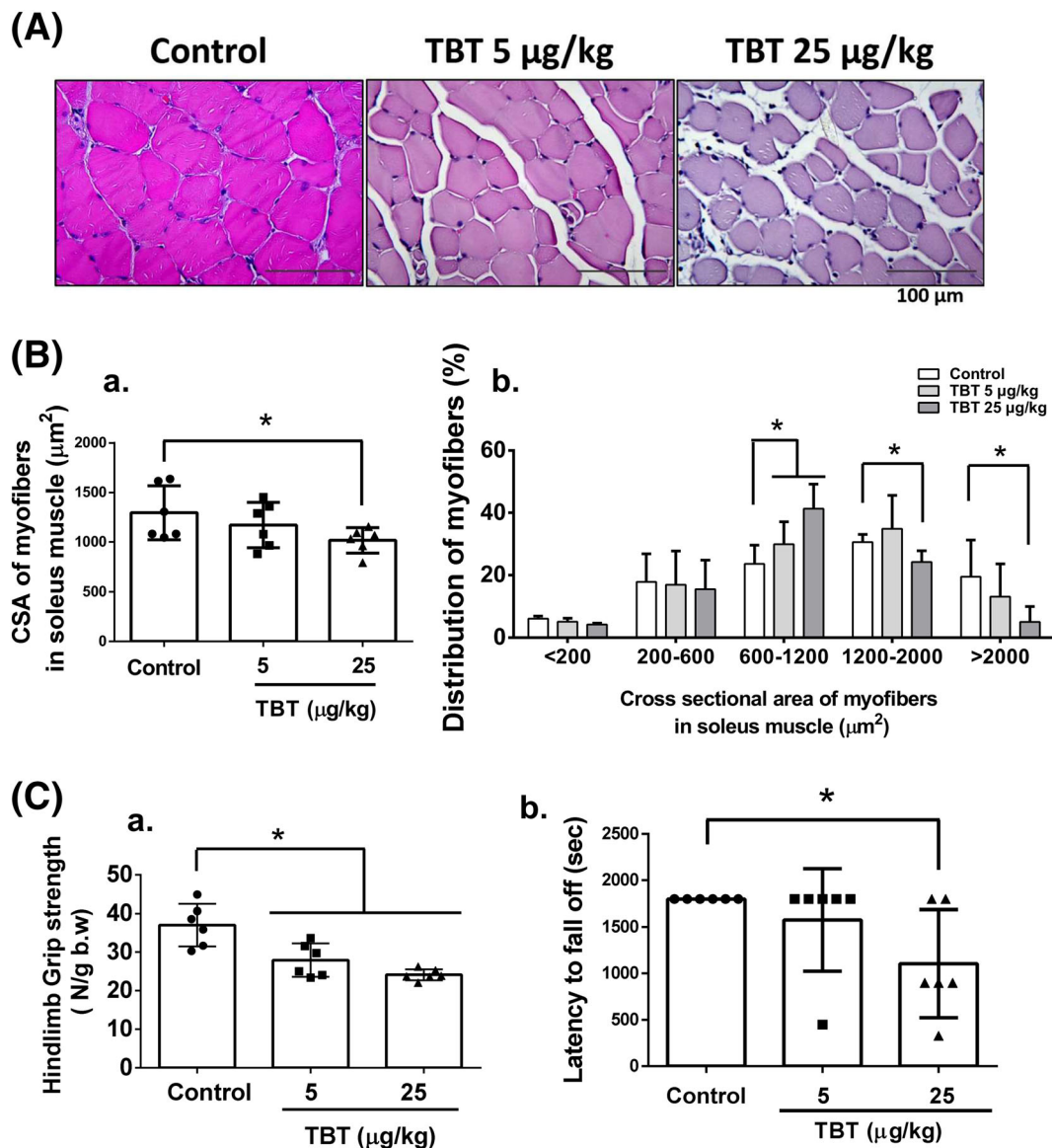


Figure 5 TBT treatment caused muscle wasting and muscular dysfunction in mice. Mice were treated with TBT (5 and 25 $\mu\text{g}/\text{kg}$) or vehicle (corn oil) for 4 weeks. (A) The representative H&E stained soleus muscle sections were shown. (B) The average cross-sectional areas (CSA) of myofibres (a) and distribution of myofibres (b) were shown. (C) The hindlimb grip strength (a) and muscle endurance in the rotarod (b) were shown. Data are presented as mean \pm SD ($n = 6$ of each group). The statistical analysis was performed using one-way ANOVA followed by unpaired two-tailed Student's *t*-test ($*P < 0.05$ compared with control group).

concentrations of 0.01–0.5 μM (10–500 nM), which were at levels of human exposure, was used to test the *in vitro* effects of TBT. Moreover, TBT at the doses of 5 and 25 $\mu\text{g}/\text{kg}/\text{day}$, which were 5 times lower than the established NOAEL and equal to NOAEL, respectively, was used to investigate the *in vivo* effects of TBT. The findings of present study demonstrated for the first time that biologically relevant dose of TBT induced muscle atrophy/wasting and retarded muscle regeneration *in vitro* and *in vivo*.

Organotin contamination not only causes adverse effects on marine organisms but also induces health risk in human

associated with contaminated seafood consumption.^{7,8,11} A cohort study showed that TBT at the levels of >0.4 ng/g fresh weight of placenta was significantly and positively associated with children's weight gain from birth to 3 months of age, suggesting that TBT may have an obesogenic potential.²⁵ A previous study has reported that TBT at a dose of 50 $\mu\text{g}/\text{kg}$ can induce the microbiome dysbiosis with obesity and dyslipidaemia in a mouse model.²⁶ TBT at a dose of 25 $\mu\text{g}/\text{kg}$ has also been found to disturb insulin regulation and glucose homeostasis in mice.¹³ Here, we found that the body weights and fasting blood glucose in mice were significantly increased

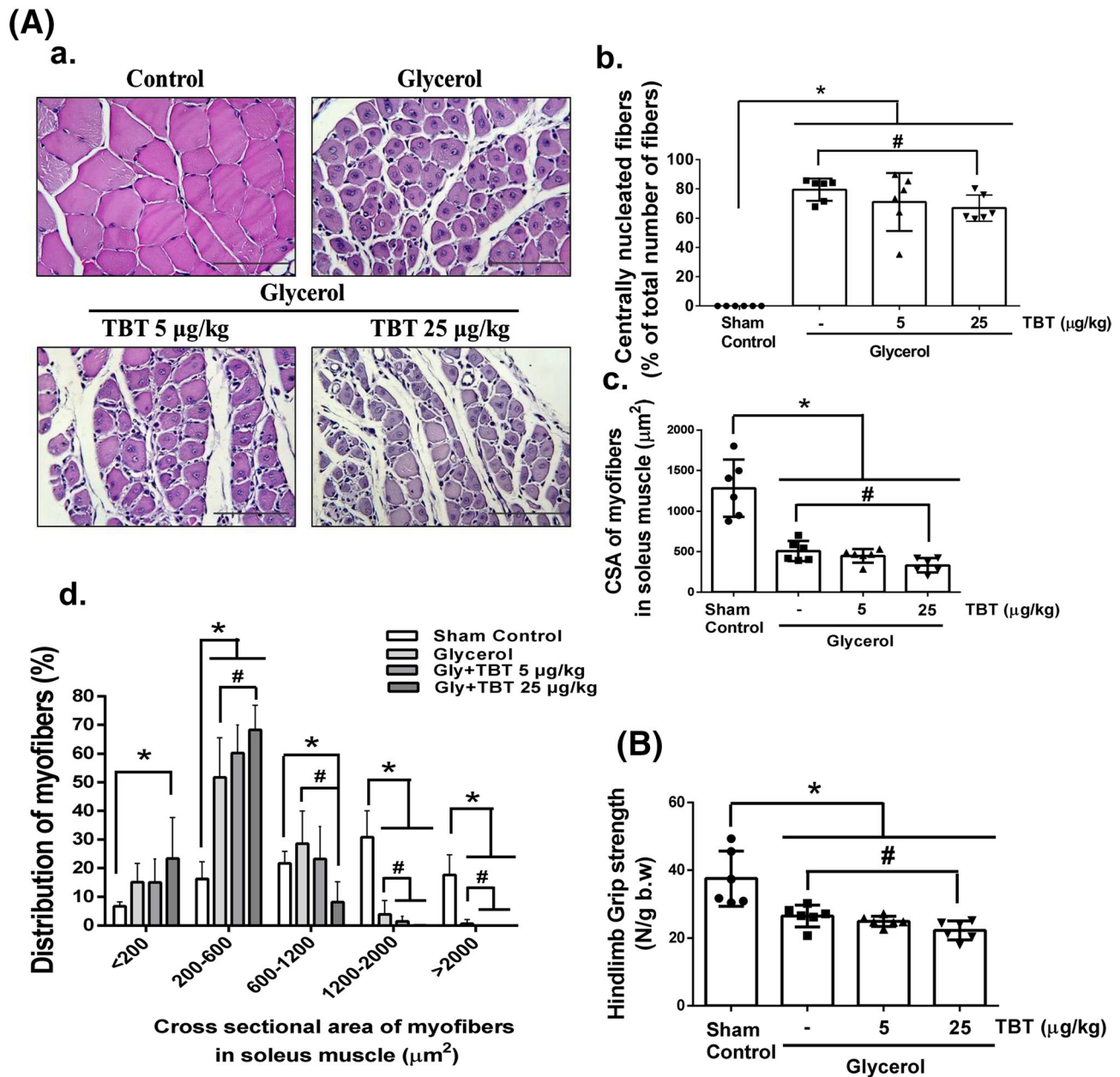


Figure 6 TBT treatment retarded muscle regeneration in mice. Mice were treated with TBT (5 and 25 µg/kg) or vehicle (corn oil) for 4 weeks. The glycerol myopathy model was used to test the effects of TBT on muscle regeneration. (A) The representative haematoxylin and eosin (H&E) stained sections of soleus muscles with glycerol-induced muscle injury (a), quantification of the percentage of soleus myofibres containing central nuclei (b), average cross-sectional areas (CSA) of myofibres (c), and distribution of myofibres (d) were shown. (B) The hindlimb grip strength was determined in TBT-treated mice after glycerol-induced muscle injury. Data are presented as mean \pm SD ($n = 6$ of each group). The statistical analysis was performed using one-way ANOVA followed by unpaired two-tailed Student's t -test (* $P < 0.05$ compared with sham control group. # $P < 0.05$ compared with glycerol group without TBT treatment).

by treatment with 25 µg/kg TBT for 4 weeks. These results are consistent with the previous findings.

In the present study, TBT administration induced muscle atrophy in soleus, tibialis anterior, and extensor digitorum longus, but not in gastrocnemius muscle, indicating that low-dose TBT-induced muscle atrophy was muscle specific,

but not muscle-type specific. The atrophy of soleus muscle, a predominantly slow-twitch muscle, is greater affected by sciatic nerve transection²⁷ and hindlimb unweighting²⁸ as compared with other calf muscles, which are mainly fast-twitch muscles. The adult soleus muscle has been found to possess more percentage of satellite cells than that in the

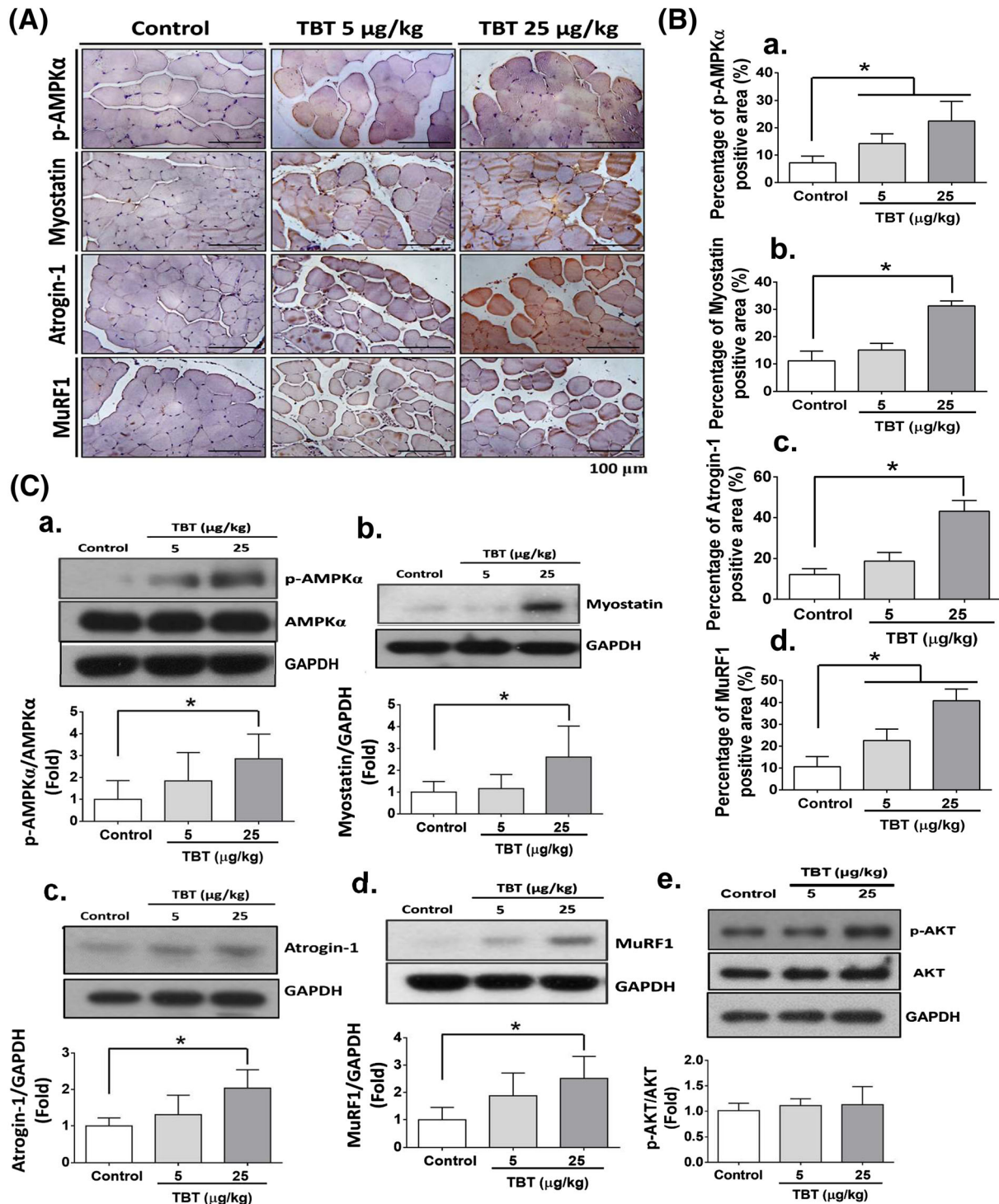


Figure 7 TBT treatment enhanced the protein expression of phosphorylated AMPK α , myostatin, Atrogin-1, and MuRF1 in the soleus muscles of mice. Mice were treated with TBT (5 and 25 $\mu\text{g}/\text{kg}$) or vehicle (corn oil) for 4 weeks. (A) The representative immunohistochemical images for the expression of phosphorylated AMPK α , myostatin, Atrogin-1, and MuRF1 were shown. Scale bar = 100 μm . (B) The quantification of protein expression for phosphorylated AMPK α (a), myostatin (b), Atrogin-1 (c), and MuRF1 (d) was shown. Data are presented as mean \pm SD ($n = 4-6$ of each group). The statistical analysis was performed using one-way ANOVA followed by unpaired two-tailed Student's t -test (* $P < 0.05$ compared with control group). (C) Effects of TBT on the protein expression of atrophy-related signalling molecules in the soleus muscles of mice. Western blot analysis for protein expression of phosphorylated AMPK α (a), myostatin (b), Atrogin-1 (c), MuRF1 (d), and phosphorylated AKT (e) in the soleus muscles of mice was shown. Data are presented as mean \pm SD ($n = 4-6$ of each group). The statistical analysis was performed using one-way ANOVA followed by unpaired two-tailed Student's t -test (* $P < 0.05$ compared with control group).

adult fast tibialis anterior and extensor digitorum longus muscles.²⁹ Therefore, we chose to target the soleus muscle for observation of muscle atrophy and regeneration in TBT-exposed mice. Moreover, in the muscle regeneration model, we injected glycerol into soleus muscles. In addition to the injury to the soleus muscle, other calf muscle (gastrocnemius and plantaris) around the soleus muscle may also be injured by infiltrated glycerol in this area, which may affect the hindlimb strength.

Diabetic hyperglycaemia can induce muscle atrophy and failure of muscle regeneration. However, the hyperglycaemic degree and duration can affect the diabetogenic effect. Recently, a study has shown that intraperitoneal injection of streptozotocin (STZ) in mice results in marked hyperglycaemia (~25 mM; equal to 450 mg/dL) for 21 days can significantly induce skeletal muscle atrophy in gastrocnemius and extensor digitorum longus muscles.²⁴ Chiu *et al.* have also observed the muscle atrophy in soleus, tibialis anterior, and gastrocnemius muscles of STZ-induced diabetic mice with blood glucose level >300 mg/dL.¹⁸ In the present study, treatment with TBT at the dose of 25 µg/kg in mice for 4 weeks only increased the blood glucose level at about 136 mg/dL, which is a weak hyperglycaemic condition, and induced muscle atrophy in soleus, tibialis anterior, and extensor digitorum longus, but not in gastrocnemius muscle. The hyperglycaemia degree or dosage may limit the effect of low-dose TBT on gastrocnemius muscle. Moreover, the current *in vitro* study also showed that TBT at low-concentrations could induce myotube atrophy. Therefore, in addition to hyperglycaemic factor, low-dose TBT, which dosage is equal to the NOAEL, may also have a direct damaging effect on skeletal muscles.

It is wondering whether TBT would affect the whole tissues, including the liver or kidney, resulting in muscle atrophy. Our preliminary data showed that TBT at the doses of 5 and 25 µg/kg did not affect the relative liver or kidney weight (Table 1) and the levels of blood liver and kidney functional markers (data not shown). Nevertheless, TBT (50 µM) exposure has been found to inhibit the Ca²⁺-dependent (homeometric) cardiac function in the intact isolated rat hearts.³⁰ TBT has also been shown to alter calcium pump activity in rat cardiac sarcoplasmic reticulum *in vitro* (0.25–10 µM) and *in vivo* (0.75–2.5 mg/kg).³¹ Compared with our study, the concentrations/doses of TBT used for inducing toxicity in the cardiac muscles are higher than that in the skeletal muscles. Moreover, TBT is known as an obesogen and diabetogen. Several studies have shown that exposure of pregnant rats to organotin caused the reduction of birth weight. The present study further investigated the adverse effects of TBT on muscle regeneration and wasting/atrophy. Therefore, oral exposure to TBT may affect functions not only in the skeletal muscles but also in other systems or organs, but with different sensitivities to the exposure doses.

AMPK is an energy sensor that serves as an important role in the maintenance of cellular homeostasis, particularly in tissues such as skeletal muscle with highly changeable energy turnover.²¹ In skeletal muscle, AMPK is known to play an important role in regulating muscle mass and regeneration.^{21,32–34} Previous studies have reported that both AICAR (an AMPK activator) and glucocorticoid dexamethasone result in myofibrillar protein degradation accompanied by AMPK-mediated upregulation and nuclear translocation of FoxO1 and FoxO3a, contributing to activation of muscle-specific E3 ubiquitin ligases Atrogin-1 and MuRF1 in C2C12-derived myotubes.³² This AICAR-induced C2C12 myotube atrophy believes to be AKT/mTOR-independent.³³ Moreover, AICAR-induced AMPK activation has also been demonstrated to suppress the myoblast differentiation and myotube formation.³⁴ These previous findings indicated that AMPK was a negative regulator for myogenesis and myotube growth under pharmacological and pathological stresses. In the present study, we also found that low-dose TBT significantly upregulated AMPK α signalling during myoblast differentiation impairment and myotube atrophy. AMPK activation upregulated Atrogin-1 and MuRF1 protein expression in myotubes and mouse soleus muscles, suggesting that AMPK signalling pathway plays an important role in TBT-induced myotube/muscle atrophy.

Skeletal muscle-derived myostatin, which is a transforming growth factor- β super-family member, can negatively regulate the muscle growth, development, and regeneration.^{22,35} Myostatin is capable of negatively regulating AKT signalling that further triggers FoxO activation and activates the ubiquitin–proteasome pathway to induce muscle protein degradation.^{22,35} The AMPK activation has been found to play an important role in enhancing the myostatin and FoxO1/3a expression in muscles of rats with exercise-induced muscle damage.³⁶ Myostatin protein expression could also be increased by AMPK activator AICAR in L6 myoblasts-derived myotubes.³⁶ Moreover, NF- κ B is a transcription factor that can also be detected in skeletal muscles under physiological and pathological atrophic conditions, such as diabetes, ageing, denervation, unloading, and sepsis.^{37,38} The pharmacological or genetic inhibition of NF- κ B has been shown to effectively prevent the denervation- or tumour-induced muscle atrophy.³⁷ The AMPK-stimulated protein degradation in skeletal muscle can also be mediated by activation of NF- κ B-regulated MuRF1/Atrogin-1 signalling pathway.³⁸ In the present study, our results showed that low-dose TBT effectively induced myostatin protein expression in C2C12 myoblasts during myogenic differentiation and differentiated C2C12 myotubes and mouse muscles. The increased protein expression of phosphorylated AMPK α and phosphorylated NF- κ B-p65 and the decreased protein expression of phosphorylated FoxO1 were also observed in myotubes and mouse soleus muscles in the presence of TBT. These findings suggest that AMPK/myostatin/FoxO1 and AMPK/NF- κ B

signalling pathways may play the important roles in TBT-induced muscle wasting/atrophy.

In this study, we found that TBT at the concentrations of 0.2 and 0.5 μM significantly decreased the AKT/mTOR phosphorylation in myotubes, which TBT-induced Atrogin-1/MuRF1 protein expression could be reversed by the AKT activator SC-79. However, the phosphorylation of AKT was not suppressed in the soleus muscles of TBT (5 and 25 $\mu\text{g}/\text{kg}$)-treated mice. The downregulation of AKT signalling has been found in advance glycation end-products (AGEs)-induced myoblast differentiation impairment and myotube atrophy.¹⁹ The Akt inactivation was shown to be involved in the arsenic-induced myoblast apoptosis.³⁹ Sandri *et al.* have shown that atrophic stress-induced AKT signalling inhibition leads to FoxO activation and Atrogin-1 induction in myotubes and muscles.²³ By contrast, Romanello *et al.* have suggested that AMPK activation amplifies FoxO action in an AKT-independent manner.³³ Further investigation for the role of AKT/mTOR signalling pathway in the TBT-induced muscle wasting is needed.

Muscle wasting has been observed in a variety of diseases, including cancer, chronic kidney disease, chronic obstructive pulmonary disease, heart failure, prolonged inactivity, and ageing, that may affect healthspan and life quality.⁴⁰ An awakening of renewed attention to skeletal muscle in recent years has prompted the discovery of new drug targets and pharmacological approaches.^{40,41} Currently, only physical exercise has been found to exhibit the positive effects in the management and prevention of muscle wasting/sarcopenia and its adverse health consequences.⁴² Therefore, the therapeutic strategies for wasting/sarcopenia still needs to be further carefully designed and studied.

In conclusions, the biologically relevant dose of TBT obviously reduces muscle mass, retards muscle regeneration, and attenuates muscular function in vitro and in vivo, suggesting TBT exposure may be an environmental risk factor for muscle regeneration inhibition, wasting/atrophy, and disease-related myopathy.

There are several study limitations: (1) The present study found that TBT administration induced muscle atrophy in soleus, tibialis anterior, and extensor digitorum longus, but not in gastrocnemius muscle. We speculated that low-dose TBT-induced muscle atrophy might be muscle specific, but not muscle-type specific. However, this speculation still needs to be further clarified. (2) There is a possibility that low-dose TBT would affect the whole tissues. This issue may be resolved in the future. (3) The serious defects may arise from EDC exposure in foetal development. It has not been explored in embryonic mice or post-natal pups following exposure of TBT to pregnant mice. This issue deserves future study.

Acknowledgements

This study was supported by grants from the Ministry of Science and Technology of Taiwan (MOST-106-2314-B-016-028; MOST-108-2314-B-016-018-MY2) and the Tri-Service General Hospital (TSGH-D-110089).

The authors certify that they complied with the ethical guidelines for authorship and publishing of the *Journal of Cachexia, Sarcopenia and Muscle*.⁴³

Conflict of interest

The authors have declared that no competing interest exists.

Online supplementary material

Additional supporting information may be found online in the Supporting Information section at the end of the article.

References

- Papalou O, Kandaraki EA, Papadakis G, Diamanti-Kandarakis E. Endocrine disrupting chemicals: an occult mediator of metabolic disease. *Front Endocrinol (Lausanne)* 2019;**10**:112.
- Park SW, Goodpaster BH, Strotmeyer ES, Kuller LH, Broudeau R, Kammerer C, et al. Accelerated loss of skeletal muscle strength in older adults with type 2 diabetes: the health, aging, and body composition study. *Diabetes Care* 2007;**30**: 1507–1512.
- Power C, Jefferis BJ. Fetal environment and subsequent obesity: a study of maternal smoking. *Int J Epidemiol* 2002;**31**:413–419.
- Street ME, Angelini S, Bernasconi S, Burgio E, Cassio A, Catellani C, et al. Current knowledge on endocrine disrupting chemicals (EDCs) from animal biology to humans, from pregnancy to adulthood: Highlights from a National Italian Meeting. *Int J Mol Sci* 2018;**19**:E1647.
- Jensen CB, Storgaard H, Madsbad S, Richter EA, Vaag AA. Altered skeletal muscle fiber composition and size precede whole-body insulin resistance in young men with low birth weight. *J Clin Endocrinol Metab* 2007;**92**:1530–1534.
- de Araújo JFP, Podratz PL, Merlo E, Sarmento IV, da Costa CS, Niño OMS, et al. Organotin exposure and vertebrate reproduction: a review. *Front Endocrinol (Lausanne)* 2018;**9**:64.
- Filipkowska A, Zloch I, Wawrzyniak-Wydrowska B, Kowalewska G. Organotins in fish muscle and liver from the Polish coast of the Baltic Sea: is the total ban successful? *Mar Pollut Bull* 2016;**111**: 493–499.
- Davies IM, McKie JC. Accumulation of total tin and tributyltin in muscle tissue of farmed Atlantic salmon. *Mar Pollut Bull* 1987;**18**:405–407.
- Fromme H, Mattulat A, Lahrz T, Rüdten H. Occurrence of organotin compounds in

- house dust in Berlin (Germany). *Chemosphere* 2005;**58**:1377–1383.
10. Kannan K, Takahashi S, Fujiwara N, Mizukawa H, Tanabe S. Organotin compounds, including butyltins and octyltins, in house dust from Albany, New York, USA. *Arch Environ Contam Toxicol* 2010;**58**:901–907.
 11. Kannan K, Senthilkumar K, Giesy JP. Occurrence of butyltin compounds in human blood. *Environ Sci Technol* 1999;**33**:1776–1779.
 12. Li B, Guo J, Xi Z, Xu J, Zuo Z, Wang C. Tributyltin in male mice disrupts glucose homeostasis as well as recovery after exposure mechanism analysis. *Arch Toxicol* 2017;**91**:3261–3269.
 13. Chen YW, Lan KC, Tsai JR, Weng TI, Yang CY, Liu SH. Tributyltin exposure at noncytotoxic doses dysregulates pancreatic β -cell function in vitro and in vivo. *Arch Toxicol* 2017;**91**:3135–3144.
 14. Adeeko A, Li D, Forsyth DS, Casey V, Cooke GM, Barthelemy J, et al. Effects of in utero tributyltin chloride exposure in the rat on pregnancy outcome. *Toxicol Sci* 2003;**74**:407–415.
 15. Cooke GM, Tryphonas H, Pulido O, Caldwell D, Bondy GS, Forsyth D. Oral (gavage), in utero and postnatal exposure of Sprague–Dawley rats to low doses of tributyltin chloride. Part 1: toxicology, histopathology and clinical chemistry. *Food Chem Toxicol* 2004;**42**:211–220.
 16. Crofton KM, Dean KF, Boncek VM, Rosen MB, Sheets LP, Chernoff N, et al. Prenatal or postnatal exposure to bis (tri-*n*-butyltin)oxide in the rat: postnatal evaluation of teratology and behavior. *Toxicol Appl Pharmacol* 1989;**97**:113–123.
 17. Penninks AH. The evaluation of data-derived safety factors for bis (tri-*n*-butyltin)oxide. *Food Addit Contam* 1993;**10**:351–361.
 18. Chiu CY, Yang RS, Sheu ML, Chan DC, Yang TH, Tsai KS, et al. Advanced glycation end-products induce skeletal muscle atrophy and dysfunction in diabetic mice via a RAGE-mediated, AMPK-down-regulated Akt pathway. *J Pathol* 2016;**238**:470–482.
 19. Chiu HC, Chiu CY, Yang RS, Chan DC, Liu SH, Chiang CK. Preventing muscle wasting by osteoporosis drug alendronate *in vitro* and in myopathy models via sirtuin-3 down-regulation. *J Cachexia Sarcopenia Muscle* 2018;**9**:585–602.
 20. Crowe AR, Yue W. Semi-quantitative determination of protein expression using immunohistochemistry staining and analysis: an integrated protocol. *Bio Protoc* 2019;**9**:e3465.
 21. Kjøbsted R, Hingst JR, Fentz J, Foretz M, Sanz MN, Pehmøller C, et al. AMPK in skeletal muscle function and metabolism. *FASEB J* 2018;**32**:1741–1777.
 22. Elkina Y, von Haehling S, Anker SD, Springer J. The role of myostatin in muscle wasting: an overview. *J Cachexia Sarcopenia Muscle* 2011;**2**:143–151.
 23. Sandri M, Sandri C, Gilbert A, Skurk C, Calabria E, Picard A, et al. FoxO transcription factors induce the atrophy-related ubiquitin ligase atrogin-1 and cause skeletal muscle atrophy. *Cell* 2004;**117**:399–412.
 24. Hirata Y, Nomura K, Senga Y, Okada Y, Kobayashi K, Okamoto S, et al. Hyperglycemia induces skeletal muscle atrophy via a WWP1/KLF15 axis. *JCI Insight* 2019;**4**:e124952.
 25. Rantakokko P, Main KM, Wohlfart-Veje C, Kiviranta H, Airaksinen R, Vartiainen T, et al. Association of placenta organotin concentrations with growth and ponderal index in 110 newborn boys from Finland during the first 18 months of life: a cohort study. *Environ Health* 2014;**13**:45.
 26. Guo H, Yan H, Cheng D, Wei X, Kou R, Si J. Tributyltin exposure induces gut microbiome dysbiosis with increased body weight gain and dyslipidemia in mice. *Environ Toxicol Pharmacol* 2018;**60**:202–208.
 27. Shen Y, Zhang Q, Huang Z, Zhu J, Qiu J, Ma W, et al. Isoquercitrin delays denervated soleus muscle atrophy by inhibiting oxidative stress and inflammation. *Front Physiol* 2020;**11**:988.
 28. Thomason DB, Booth FW. Atrophy of the soleus muscle by hindlimb unweighting. *J Appl Physiol* 1985;**1990**:1–12.
 29. Chargé SB, Rudnicki MA. Cellular and molecular regulation of muscle regeneration. *Physiol Rev* 2004;**84**:209–238.
 30. Pereira CLV, Ximenes CF, Merlo E, Sciortino AS, Monteiro JS, Moreira A, et al. Cardiotoxicity of environmental contaminant tributyltin involves myocyte oxidative stress and abnormal Ca^{2+} handling. *Environ Pollut* 2019;**247**:371–382.
 31. Kodavanti PR, Cameron JA, Yallapragada PR, Vig PJ, Desai D. Inhibition of Ca^{2+} transport associated with cAMP-dependent protein phosphorylation in rat cardiac sarcolemmal reticulum by triorganotins. *Arch Toxicol* 1991;**65**:311–317.
 32. Nakashima K, Yakabe Y. AMPK activation stimulates myofibrillar protein degradation and expression of atrophy-related ubiquitin ligases by increasing FOXO transcription factors in C2C12 myotubes. *Biosci Biotechnol Biochem* 2007;**71**:1650–1656.
 33. Romanello V, Guadagnin E, Gomes L, Roder I, Sandri C, Petersen Y, et al. Mitochondrial fission and remodelling contributes to muscle atrophy. *EMBO J* 2010;**29**:1774–1785.
 34. Williamson DL, Butler DC, Alway SE. AMPK inhibits myoblast differentiation through a PGC-1 α -dependent mechanism. *Am J Physiol Endocrinol Metab* 2009;**297**:E304–E314.
 35. Carnac G, Vernus B, Bonnieu A. Myostatin in the pathophysiology of skeletal muscle. *Curr Genomics* 2007;**8**:415–422.
 36. Lee K, Ochi E, Song H, Nakazato K. Activation of AMP-activated protein kinase induce expression of FoxO1, FoxO3a, and myostatin after exercise-induced muscle damage. *Biochem Biophys Res Commun* 2015;**466**:289–294.
 37. Cai D, Frantz JD, Tawa NE Jr, Melendez PA, Oh BC, Lidov HG, et al. IKK β /NF- κ B activation causes severe muscle wasting in mice. *Cell* 2004;**119**:285–298.
 38. Egawa T. Participation of AMPK in the control of skeletal muscle mass. In Sakuma K, ed. *The plasticity of skeletal muscle*. Singapore: Springer; 2017. p 251–275.
 39. Yen YP, Tsai KS, Chen YW, Huang CF, Yang RS, Liu SH. Arsenic induces apoptosis in myoblasts through a reactive oxygen species-induced endoplasmic reticulum stress and mitochondrial dysfunction pathway. *Arch Toxicol* 2012;**86**:923–933.
 40. Furrer R, Handschin C. Muscle wasting diseases: novel targets and treatments. *Annu Rev Pharmacol Toxicol* 2019;**59**:315–339.
 41. Lynch GS. Identifying the challenges for successful pharmacotherapeutic management of sarcopenia. *Expert Opin Pharmacother* 2022;**23**:1233–1237.
 42. Liguori I, Russo G, Aran L, Bulli G, Curcio F, Della-Morte D, et al. Sarcopenia: assessment of disease burden and strategies to improve outcomes. *Clin Interv Aging* 2018;**13**:913–927.
 43. von Haehling S, Morley JE, Coats AJS, Anker SD. Ethical guidelines for publishing in the Journal of Cachexia, Sarcopenia and Muscle: update 2021. *J Cachexia Sarcopenia Muscle* 2021;**12**:2259–2261.